

Real-time Display and *In-vivo* Optical-resolution Photoacoustic Microscopy for Ophthalmic Imaging

Sang-Won Lee^{1,2,3}, Heesung Kang¹ and Tea Geol Lee^{1,2}

¹Center for Nano-Bio Measurement, Korea Research Institute of Standards and Science, Daejeon, Rep. of Korea

²Department of Nano Science, University of Science and Technology, Daejeon, Rep. of Korea

³Center for Nanosafety Metrology, Korea Research Institute of Standards and Science, Daejeon, Rep. of Korea

Keywords: Optical-resolution Photoacoustic Microscopy, Ophthalmic Imaging, Angiography.

Abstract: Photoacoustic imaging is a non-invasive imaging technology that can be combined with optical absorption contrast and detection of acoustic wave for structural, functional, and molecular imaging. Especially, optical-resolution photoacoustic microscopy (OR-PAM) can provide a high spatial resolution with a micron-scale. In this study, we have developed laser-scanning OR-PAM, which could obtain *in-vivo* photoacoustic ophthalmic angiography. For high speed image acquisition, we used a nanosecond pulsed laser with a 300 kHz-pulse repetition rates. In addition, we carried out parallel signal processing using a graphics processing unit to enable fast signal processing. Therefore, we successfully obtained maximum amplitude projection images of microvasculature in anterior and posterior segments of mouse's eye with real-time display of 0.98 fps.

1 INTRODUCTION

Most of the imaging modalities in ophthalmology, such as fundus camera (Pomerantzeff et al., 1979), slit-lamp, scanning laser ophthalmoscope (Webb and Hughes, 1981), and optical coherence tomography (Huang et al., 1991), are based on detection of reflected light or single-backscattered light (Jiao et al., 2010). These imaging techniques have advantages that can provide anatomical and functional images for noninvasively accurate diagnosis of ocular diseases. Optical coherence tomography (OCT) cannot provide only three-dimensional and structural images but also label-free functional images such as Doppler (Chen et al., 1997), polarization (Ren et al., 2002), and angiography (Wang et al., 2007). Additionally, fundus camera and scanning laser ophthalmoscope (SLO) can image retinal vasculature with high transverse resolution using contrast agents such as fluorescein and indocyanine green (Song et al., 2013). However, these optical imaging tools cannot support information of the molecules with optical absorption properties in ocular tissues.

Photoacoustic imaging combined with optical absorption contrast and detection of acoustic wave has been actively studied because photoacoustic imaging can provide structural, functional, and

molecular images (Wang et al., 2003, Zhang et al. 2006, Kim et al., 2010). Especially, optical-resolution photoacoustic microscopy (OR-PAM) can provide microscopic images with high spatial resolution using tightly focused laser spot with a micro-scale (Maslov et al. 2008, Xie et al. 2009)

Recently, several groups have developed ophthalmic photoacoustic microscopy (Jiao et al., 2010, Hu et al., 2010, de la Zerda et al., 2010, Silverman et al., 2010). Hu et al. and de la Zerda et al. have demonstrated ocular OR-PAM images with an acquisition speed of a few hours owing to usages of a low pulse repetition rate laser and mechanical scanning (Hu et al., 2010, de la Zerda et al. 2010). Silverman et al. could achieve the imaging speed with 2.7 s for volumetric acquisition (Silverman et al., 2010). However, their image pixel size was limited to be 256 × 256 pixels. The imaging speed in OR-PAM depends on the pulse repetition rate of the laser and an acquired image pixel size.

The higher acquisition speed for an ophthalmic image is important to reduce motion artifacts by breathing, heartbeat, and eye movements. In addition, small image pixel size can cause a low image pixel resolution at the large field of view (FOV) although an optical resolution by a tightly focused beam size is very small.

In our previous study, we have demonstrated maximum amplitude projection (MAP) images of blood vessels in a mouse's ear from volumetric data set with the data size of $736 \times 500 \times 500$ points at 1.02 seconds (Kang et al., 2015). For high speed image acquisition, we used a nanosecond pulsed laser with a pulse repetition rate of 300 kHz and carried out parallel signal processing with graphics processing unit (GPU).

In this study, we modified and applied our high-speed laser-scanning OR-PAM system to obtain photoacoustic ophthalmic images. Therefore, we could obtain MAP images of microvasculature in anterior and posterior segments of mouse's eye with real-time display of 0.98 fps and large pixel size of 500×500 pixels.

2 EXPERIMENTAL METHODS

2.1 Laser-Scanning OR-PAM

Figure 1 shows a schematic diagram of a laser-scanning OR-PAM. This schematic was modified from our previous study (Kang et al., 2015). We used an Ytterbium-doped fiber laser (YLP-G10, IPG Photonics Corp.) with 1-ns pulse width and 300-kHz pulse repetition rates at 532 nm. Light from the laser was delivered by an optical fiber and scanned by 2-D galvanometer scanning mirror with silver coating

(GVSM002, Thorlabs Inc.) as shown in Fig. 1 (a). In our previous study, collimated light was scanned and focused in inverse direction (bottom-to-top). In addition, the acoustic waves were detected in direction pass through a sample with optical path as shown in Fig. 1(b). This schematic could obtain OR-PAM images of blood vessels in mouse's ear because thickness of mouse's ear is thin below $500 \mu\text{m}$.

However, in the eye, we could not apply acoustic wave detection method in transmitted direction. Therefore, we used a schematic of Fig. 1 (c) that the acoustic waves occurred at the focal plane were reflected by a thin glass with a tilting angle of 45° in a water tank. Reflected acoustic wave detected by ultrasound transducer. Finally, detected signals were amplified by a pulser/receiver (5072PR, Olympus-NDT) and digitally converted by a high-speed digitizer (ATS9350, AlazarTech) at a sampling rate of 250 MSamples/s.

For fast signal processing and real-time display, we carried out parallel signal processing using GPU. A graphics card (ASUS GTX780Ti, ASUSTeK Computer Inc.) for GPU processing has 2880 stream processors, a 7000 MHz memory clock and 3 GB of RAM. To accelerate signal processing time and display real-time OR-PAM images, we developed custom software using Visual C++ of Visual Studio 2012 (Microsoft) and compute unified device architecture (CUDA) technology (NVIDIA Corp.).

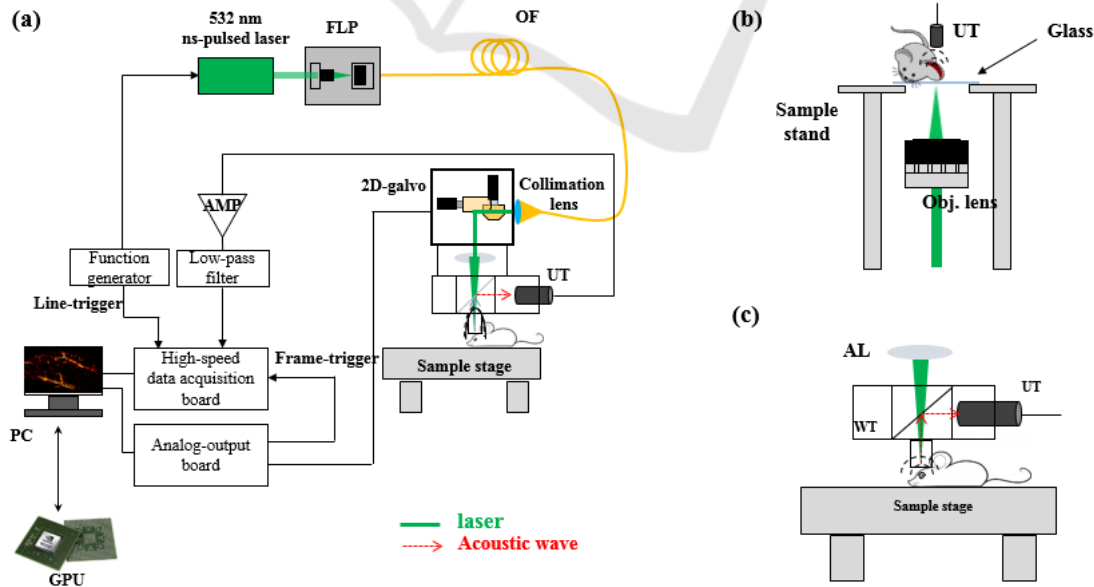


Figure 1: (a) Schematic diagram of laser-scanning OR-PAM for ophthalmic imaging, (b) previous our setup for light illumination and acoustic wave detection, (c) modified setup for light illumination and acoustic wave detection.

2.2 Animal Preparation

We used BALB/c mice at 6 ~ 8 weeks of age as an animal experiment model. The mice were housed under standard conditions (room temperature $23\pm 2^\circ\text{C}$, humidity $50\pm 10\%$) with a 12-h dark-light cycle and were fed standard laboratory chow and water ad libitum. The care, use, and interventions were approved by the Korea Research Institute of Bioscience and Biotechnology (KRIBB). Before retinal imaging, mydriatic was applied to dilate the pupil. During imaging, the anesthetized mice were restrained in a customized holder.

3 RESULTS AND DISCUSSION

The volumetric data set was obtained at the laser pulse repetition rate of 300 kHz and composed with 736 points per line, 500 lines per B-mode-frame, and 500 B-mode-frames per C-mode-frame. Therefore, data size per volume was 351 MB (2 bytes \times 736 \times 500 \times 500). In previous study, when we carried out signal processing without parallel processing using GPU, the total processing time was approximately 31.2 s. However, we could accelerate the processing time to 1.02 s using parallel processing using GPU.

To evaluate the transverse resolution of our OR-PAM system, we obtained the MAP image of a USAF 1951 resolution target (Edmunds Optics) as a sample. When an area $3\text{ mm} \times 3\text{ mm}$ was achieved as the maximum FOV, the lines at group 5 and element 6 could be distinguished. Therefore, a lateral resolution was measured to be approximately $17.5\ \mu\text{m}$. In addition, when the FOV was reduced to $1\text{ mm} \times 1\text{ mm}$, we could distinguish the lines at group 7 and element 1, corresponding to a lateral resolution of $7.8\ \mu\text{m}$ (Kang et al., 2015). This difference of the lateral resolution came results from changing an image pixel resolution owing to sizes of FOV rather than a spot size of focused beam.

Figure 2 shows the MAP image (a) and 3-D volumetric rendering image (b) of microvasculature in the iris of a BALB/c mouse. When the microvasculature image was obtained, a focused ultrasound transducer at the center frequency of 20 MHz (V317-SU-F1.00in-PTF, Olympus-NDT) was used. Focused ultrasound transducer had a -6 dB bandwidth of 42.21%. In the anterior segment, the vessels in the iris can be seen clearly in the MAP image as shown in Fig. 2 (a). In addition, the location of the pupil was well displayed as a hole at the center

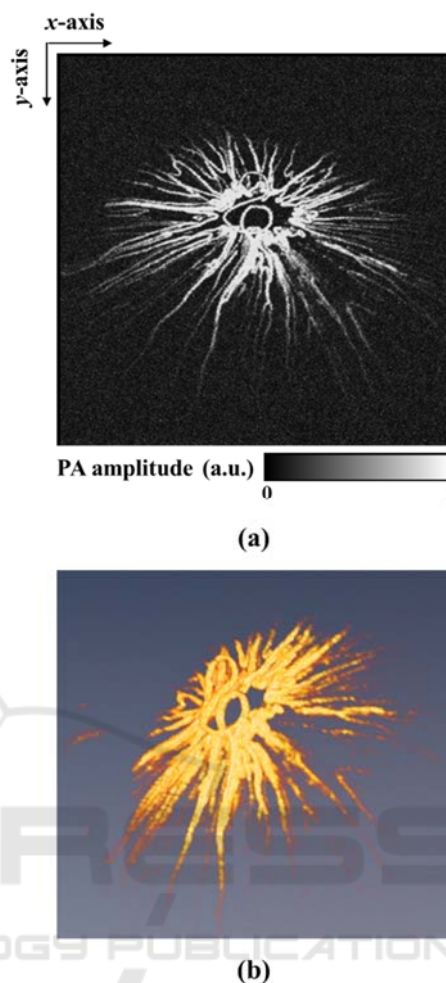


Figure 2: *In-vivo* photoacoustic ophthalmic angiography of the iris microvasculature of a BALB/c mouse. (a) MAP image and (b) 3-D rendering image.

of the iris. Figure 2 (b) was processed with Amira 6.1 (FEI Corp.).

Figure 3 shows MAP images of retinal vasculature (a) and sclera choroidal vasculature (b), respectively. We used an unfocused ultrasound transducer at the center frequency of 15 MHz when the vasculature images in the posterior segment of the mouse's eye was acquired. In previous paper, light with a pulse energy of 500 nJ was illuminated to image a posterior eye using focused laser beam (Wu et al., 2014). In this study, we used a pulse energy of approximately 600 nJ. As shown in Fig. 3 (a), we could clearly observed that blood vessels in the retina were gathered into optic disk area (red arrow). When the focal position of light was shifted onto deeper area and the incident angle of light was adjusted, we could obtain the choroidal vascular (red arrows) image in

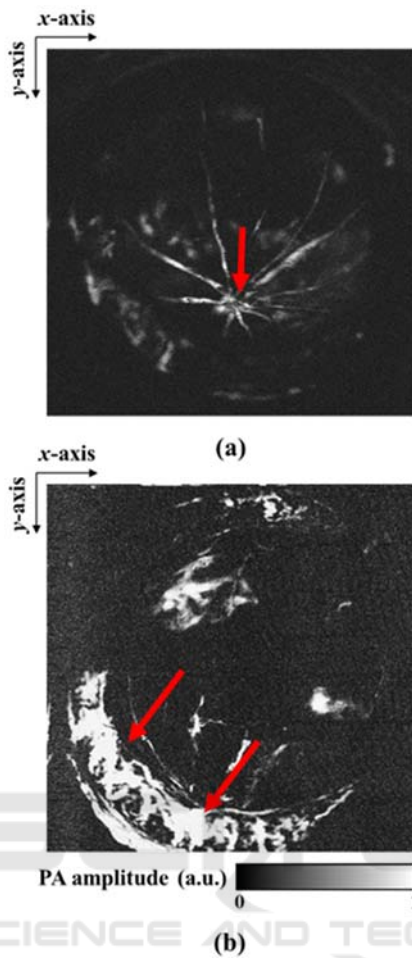


Figure 3: *In-vivo* photoacoustic ophthalmic angiography of the posterior segment of a BLAB/c mouse. (a) Retinal vasculature and (b) sclera choroidal vasculature.

mouse's sclera as shown in Fig. 3 (b).

PAM have been studied as useful molecular imaging tool with contrast agents in various medical fields. PAM will be also used as a preclinical imaging tool in ophthalmology for drug development and diagnosis of disease targeted with specific receptors such as the vascular endothelial growth factor using nanoparticles or dyes. In addition, if PAM is combined with various ophthalmic imaging tools (OCT, fundus, and SLO), we can obtain structural, functional, and molecular information.

4 CONCLUSIONS

In conclusion, we demonstrated real-time display photoacoustic ophthalmic angiography using laser-scanning OR-PAM at a mouse's anterior and

posterior segment. We could display MAP images with 500×500 pixels as volumetric images at 0.98 fps when we used a nanosecond pulse laser with 300-kHz pulse repetition rates. In further study, we will obtain molecular images to apply diagnosis of ocular disease using bio-conjugated contrast agents, which are based on optical absorbance such as nanoparticles and dyes.

ACKNOWLEDGEMENTS

This work was supported by the "Development of Platform Technology for Innovative Medical Measurement Program (KRIS-2016-16011064)" from the Korea Research Institute of Standards and Science. It was also supported by grants from the "Pioneer Research Center Program (2012-0009541)" and the "Nano Material Technology Development Program (2014M3A7B6020163)" through the National Research Foundation (NRF), Rep. of Korea.

REFERENCES

- Chen, Z., Milner, S. S., Wang, X., Malekafzali, A., van Germent, M. J. C., & Nelson, J. S., 1997. Noninvasive imaging of in vivo blood flow velocity using optical Doppler tomography. *Optics Letters*, 22, 1119-21.
- de la Zerda, A., Paulus, Y. M., Teed, R., Bodapati, S., Dollberg, Y., Khuri-Yakub, B. T., Blumenkranz, M. S., Moshfeghi, D. M. & Gambhir, S. S., 2010. Photoacoustic ocular imaging. *Optics Letters*, 35, 270-2.
- Hitenberger, C. K., Götzinger, E., Stricker, M., Pircher, M., & Fercher, A. F., 2001. Measurement and imaging of birefringence and optic axis orientation by phase resolved polarization sensitive optical coherence tomography, *Optics Express*, 9, 780-90.
- Hu, S. Rao, B., Maslov, K. & Wang, L. V., 2010. Label-free photoacoustic ophthalmic angiography. *Optics Letters*, 35, 1-3.
- Huang, D., Swanson, E. A., Lin, C. P., Schuman, J. S., Stinson, W. G., Chang, W., Hee, M. R., Flotte, T., Gregory, K., Puliafito, C. A. & Fujimoto, J. G., 1991. Optical coherence tomography. *Science*, 245, 1178-81.
- Jiao, S., Jiang, M. Hu, J., Fawzi, A., Zhou, Q., Shung, K. K., Puliafito, C. A. & Zhang, H. F., 2010. Photoacoustic ophthalmoscopy for in vivo retinal imaging. *Optics Express*, 18, 3967-72.
- Kang, H., Lee, S. W., Lee, E. S., Kim, S. H. & Lee, T. G., 2015. Real-time GPU-accelerated processing and volumetric display for wide-field laser-scanning optical-resolution photoacoustic microscopy. *Biomedical Optics Express*, 6, 4650-60.

- Kim, C., Cho, E. C., Chen, J. Song, K. H., Au, L., Favazza, C., Zhang, Q., Cobley, C. M., Gao, F., Xia, Y. & Wang, L. V., 2010. In vivo molecular photoacoustic tomography of melanomas targeted by bioconjugated gold nanocages. *ACS Nano*, 4, 4559-64.
- Maslov, K., Zhang, H. F., Hu, S. & Wang, L. V., 2008. Optical-resolution photoacoustic microscopy for in vivo imaging of single capillaries. *Optics Letters*, 33, 929-31.
- Pomerantzeff, O., Webb, R. H. & Delori, F. C., 1979. Image formation in fundus cameras. *Invest Ophthalmol Vis Sci*, 18, 630-7.
- Silverman, R. H., Kong, F., Chen, Y. C., Lloyd, H. O., Kim, H. H., Cannata, J. M., Shung K. K. & Coleman, D. J., 2010. High-resolution photoacoustic imaging of ocular tissues. *Ultrasound in Medicine & Biology*, 36, 733-42.
- Song, W., Wei, Q., Feng, L. Sarthy, V. Jiao, S. Liu, X. & Zhang, H. F., 2003. Multimodal photoacoustic ophthalmoscopy in mouse, *Journal of Biophotonics*, 6, 505-12.
- Wang, R. K., Jacques, S. L., Ma, Z., Hurst, S. Hanson, S. R. & Gruber, A. Three dimensional optical angiography. *Optics Express*, 15, 4083-97.
- Wang, X., Pang, Y., Ku, G., Xie, X. Stoica, G. & Wang, L. V., 2003. Noninvasive laser-induced photoacoustic tomography for structural and functional in vivo imaging of the brain. *Nature Biotechnology*, 21, 803-6.
- Webb, R. H. & Hughes, G. W., 1981. Scanning laser ophthalmoscope. *IEEE Trans Biomed Eng*, 28, 488-92.
- Wu, N., Ye, S., Ren, Q. & Li, C., 2014. High-resolution dual-modality photoacoustic ocular imaging. *Optics Letters*, 39, 2451-4.
- Xie, Z., Jiao, S., Zhang, H. F. & Puliafito, C. A., 2009. Laser-scanning optical-resolution photoacoustic microscopy. *Optics Letters*, 34, 1771-3.
- Zhang, H. F., Maslov, K., Stoica, G. & Wang, L. V., 2006. Functional photoacoustic microscopy for high-resolution and noninvasive in vivo imaging. *Nature Biotechnology*, 24, 848-51.